

# Relative Permittivities of 1,1,1,2,3,3,3-Heptafluoropropane (HFC-227ea), 1,1,1,2,3,3-Hexafluoropropane (HFC-236ea), and 1,1,1,3,3-Pentafluorobutane (HFC-365mfc) in the Liquid Phase

A. P. C. Ribeiro,<sup>†</sup> C. A. Nieto de Castro,<sup>\*,†,‡</sup> R. S. Pai-Panandiker,<sup>†,§</sup> and U. V. Mardolcar,<sup>†,#</sup>

Centro de Ciências Moleculares e Materiais and Departamento de Química e Bioquímica, Faculdade de Ciências da Universidade de Lisboa, Campo Grande, 1749-016 Lisboa, Portugal, and Instituto Superior Técnico, Departamento de Física e Nucleo de Termofísica, Av. Rovisco Pais, 1049-001 Lisboa, Portugal

Relative permittivity measurements of 1,1,1,2,3,3,3-heptafluoropropane (HFC-227ea), 1,1,1,2,3,3-hexafluoropropane (HFC-236ea), and 1,1,1,3,3-pentafluorobutane (HFC-365mfc) in the liquid phase are reported. Measurements were performed by using a direct capacitance method at temperatures from 223 K to 303 K and pressures up to 16 MPa for HFC-227ea and HFC-236ea and at temperatures from 263 K to 303 K up to 16 MPa for HFC-365mfc. The uncertainty of the relative permittivity measurements is estimated to be better than  $\pm 1.1 \cdot 10^{-2}$ . The theory developed by Vedam et al., and adapted by Diguet, and the Kirkwood modification of the Onsager were applied to obtain the apparent dipole moment of HFC-227ea, HFC-236ea, and HFC-365mfc in the liquid state, found to be 2.356 D for HFC-227ea, 2.624 D for HFC-236ea, and 4.917 D for HFC-365mfc. The effective dipole in the liquid state of HFC-236ea predicted by the Kirkwood–Frölich theory is 2.065 D. Density functional and density functional self-consistent calculations (SCIPCM) of the electronic distribution and of the dipole moment are reported for HFC-227ea.

## Introduction

It is widely accepted that the chlorine-containing compounds (CFCs and HCFCs) are the source of ozone depletion in Earth's atmosphere and contribute to the greenhouse effect. Replacement of these compounds by new alternative refrigerants, chlorine free, usually named HFCs, needs the value of the thermophysical properties of this new compounds, chosen with regard to their values of the ozone depletion potential (ODP) and global warming potential (GWP). HFC-227ea (1,1,1,2,3,3,3-heptafluoropropane) and HFC-236ea (1,1,1,2,3,3-hexafluoropropane) are recently introduced, commercially available hydrofluorocarbons useful in fire suppression, sterilization, propellant applications, and refrigeration (ODP = 0). They can also be used as alternatives to Halons, HCFC-22, R502, and CFC-114.

Thermophysical property data were already obtained for HFC-227ea including vapor pressure, density, calorimetric data, viscosity, thermal conductivity, speed of sound, and surface tension in the liquid state, helping to develop an equation of state (EOS).<sup>1–4</sup> For HFC-236ea available measurements include refractive index, speed of sound in the vapor phase, density, surface tension in the vapor phase, relative permittivity, the dipole moment in the vapor phase, and VLE measurements.<sup>5–11</sup> HFC-365mfc (1,1,1,3,3-pentafluorobutane) is a third-generation substitute for fully and partially halogenated

chlorofluorohydrocarbons. It is flammable and has a wide range of applications in the field of plastic foams, due to its good physical properties. HFC-365mfc forms azeotropes with pentanes, improving the properties of hydrocarbon blow foams. HFC-365mfc measurements include compressed and saturated liquid densities, vapor phase thermal conductivity, and vapor pressure.<sup>12,13</sup>

Recent advances in the understanding of the polar interactions in the gas and liquid phases showed the extreme importance of the electric properties of these polar fluids, which can give insight to the molecular theory of liquids. Additionally, the data are fundamental for the design of machinery used in the air-conditioning and refrigeration industry. Relative permittivity provides information about the behavior of the molecules under an electrical field, controlled by their chemical structure and molecular interactions.<sup>14</sup>

More recent studies of the measurement of the relative permittivity in the liquid state and the interpretation of neutron-scattering spectral data in conjunction with molecular dynamics simulations have been attempted to elucidate the liquid-state structure of these systems. The present calculations of the electronic distribution and of the dipole moment in the liquid state were based on the density functional theory. The approach developed was published recently.<sup>15</sup>

As a continuation of our previous work,<sup>14</sup> we have studied the dependence of the relative permittivity on density, applying the concept of Eulerian deformation, also named Eulerian strain, based on the work of Vedam et al.<sup>16,17</sup> and Diguet.<sup>18</sup> In addition, to contribute to a better understanding of the structure of polar liquids, the apparent dipole moment in the liquid phase was estimated by applying the theory of molecular polarizability developed by Kirkwood<sup>19</sup> on the basis of the definition of Onsager's local field<sup>20</sup> and further modified by Frölich.<sup>21</sup>

\* Author to whom correspondence should be addressed. E-mail: cacastro@fc.ul.pt.

<sup>†</sup> Centro de Ciências Moleculares e Materiais, Faculdade de Ciências da Universidade de Lisboa.

<sup>‡</sup> Departamento de Química e Bioquímica, Faculdade de Ciências da Universidade de Lisboa.

<sup>§</sup> Present address: The Boston Consulting Group, Rua das Chagas 7-15, 1200-106 Lisboa, Portugal.

<sup>#</sup> Instituto Superior Técnico, Departamento de Física e Nucleo de Termofísica.

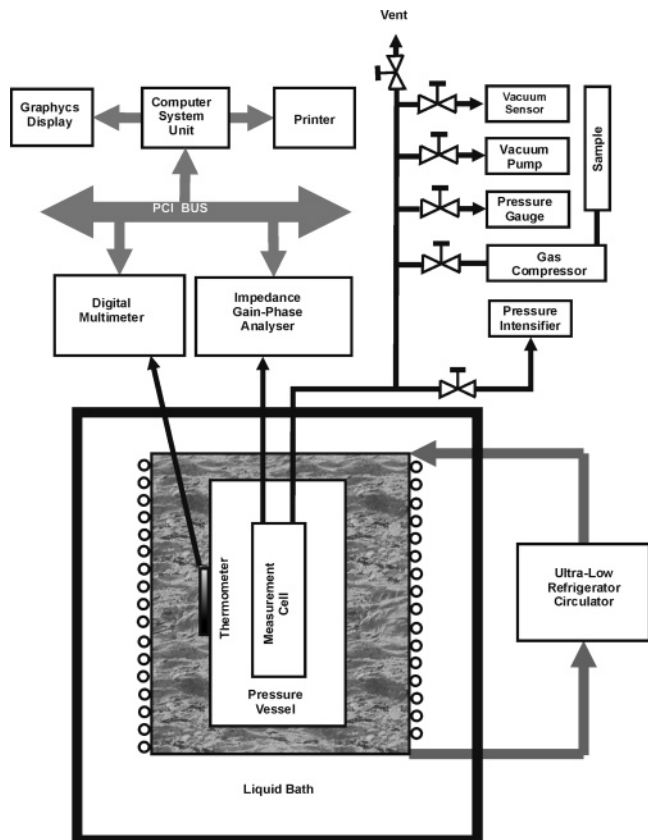


**Figure 1.** Schematic diagram of the apparatus. The figure is self-contained.

## Experimental Section

The experimental setup is based on a three-terminal arrangement and the relative permittivity,  $\epsilon_r$ , was obtained from the ratio between the ratio of the capacitances of the cell with the sample and under vacuum. The instrument has been thoroughly documented in earlier publications<sup>22–24</sup> and is described only briefly here. The capacitance of the cell was measured in an absolute mode using an impedance analyzer (Schlumberger, type SI 1260) with a precision of  $\pm 5 \cdot 10^{-4}$  pF. The capacitance of the cell under vacuum was approximately 5.7 pF. The temperature was measured with a calibrated platinum resistance thermometer with an accuracy of 5 mK. The pressure vessel was immersed in a circulating flow thermostat bath with a stability of 10 mK during 1 h. A cryostat provided the circulating liquid. Pressure was measured with a pressure transducer with a precision of 0.01 MPa. The schematic diagram of the apparatus setup<sup>24</sup> for the measurements of the relative permittivity in the liquid phase is presented in Figure 1.

The sample of HFC-227ea was provided by Ausimont S.p.A. with a purity of 99.9 %, the HFC-236ea sample was provided

by Lancaster Inc. (99 % purity), and the HFC-365mfc sample was produced by Solvay Fluor und Derivate GmbH (purity >99.5 %). The samples were used without further purification. Table 1 describes the purity and other physical properties of the liquids studied.

The measurements were performed at an average of nine isotherms separated by  $\approx 10$  K for HFC-227ea and HFC-236ea and five isotherms separated by  $\approx 10$  K for HFC-365mfc, in steps of 1 MPa, from 1 MPa to 16 MPa. The repeatability of the measurements was found to be of the order of 0.01 %, and the uncertainty is estimated to be better than  $\pm 1.1 \cdot 10^{-2}$  for a confidence interval of 95 % (ISO definition,  $k = 2$ ). The density values of these refrigerants were calculated using the REFPROP database, version 7,<sup>25</sup> except for HFC-365mfc, for which they were calculated with the equation of state of Lemmon et al.,<sup>26</sup> with an average uncertainty of 0.16 %.

For HFC-227ea was developed a density functional theory approach and a self-consistent reaction for comparison with the experimental calculated results.<sup>15</sup> The effective dipole in the liquid phase ( $\mu^*_{KF}$ ) for HFC-236ea was predicted by the Kirkwood–Frölich equation, where the refractive index ( $n$ ) has been calculated for the condensed phase.<sup>27</sup>

## Results

The relative permittivity of the fluid,  $\epsilon_r$ , can be calculated from the ratio of the capacitance between the capacitance,  $C(P, T)$ , at pressure  $P$  and temperature  $T$  and the capacitance,  $C_0(T)$ , under vacuum. (The relative permittivity,  $\epsilon_r$ , is defined as the ratio between the permittivity of the fluid,  $\epsilon$ , and the permittivity of a vacuum,  $\epsilon_0$ .) Table 2 presents the data obtained as a function of pressure and density for each isotherm, for HFC-227ea,  $T_n$  being a nominal temperature. Table 3 shows the data for HFC-236ea and Table 4 the data for HFC-365mfc. All of the experimental points measured at a given temperature,  $T$ , close to  $T_n$ , were adjusted to this temperature using the following relationship:

$$\epsilon_r(T_n, P) = \epsilon_r(T, P) + \left( \frac{\partial \epsilon_r}{\partial T} \right)_P (T_n - T) \quad (1)$$

The results were expressed as functions of temperature and pressure or density. Figures 2 and 3 show the relative permittivity as a function of density for HFC-227ea and HFC-236ea, for all of the nominal temperatures. The relative permittivity as a function of density, for HFC-365mfc, is shown in Figure 4. The behavior is qualitatively identical for all of the pure fluids, as  $(\partial \epsilon_r / \partial P)_T$  is positive and  $(\partial \epsilon_r / \partial T)_P$  is negative. However,  $(\partial \epsilon_r / \partial \rho)_T$  is always positive.

The experimental data of the relative permittivity were fitted by a maximum likelihood iterative  $\chi^2$  method for a multiparameter and multivariable function in density and temperature

**Table 1. Physical Properties and Purity of the Hydrofluorocarbons**

	1,1,1,2,3,3-heptafluoropropane	1,1,1,2,3,3-hexafluoropropane	1,1,1,3,3-pentafluorobutane
ASHRAE nomenclature	R-227ea	R-236ea	R-365mfc
molecular formula	$\text{CF}_3\text{CHFCF}_3$	$\text{CF}_3\text{CHFCHF}_2$	$\text{CF}_3\text{CH}_2\text{CF}_2\text{CH}_3$
relative molar mass/g·mol <sup>-1</sup>	170.03	152.04	148.07
ODP (CFC-11 = 1)	0	0	0
GWP <sup>a</sup> ( $\text{CO}_2 = 1$ )	2900	0.35	0.21
boiling point @1atm/°C	-15.6	6.19	41.35
estimated water content /ppm	33.5	30	15
purity	99.9 %	99.9 %	> 99.5 %
sample provider	Ausimont S.p.A., Italy	Lancaster Inc., USA	Solvay Fluor und Derivate, GmbH, Germany

<sup>a</sup> Integrated time horizon = 100 years.

**Table 2.** Relative Permittivity  $\epsilon_r$  of HFC-227ea, from  $T = 223.15\text{ K}$  to  $303.15\text{ K}$  and up to  $P = 16\text{ MPa}$ 

$T/\text{K}$	$P/\text{MPa}$	$\rho/\text{kg}\cdot\text{m}^{-3}$	$\epsilon_r(T, P)$	$\rho(T_n, P)/\text{kg}\cdot\text{m}^{-3}$	$\epsilon_r(T_n, P)$	$T/\text{K}$	$P/\text{MPa}$	$\rho/\text{kg}\cdot\text{m}^{-3}$	$\epsilon_r(T, P)$	$\rho(T_n, P)/\text{kg}\cdot\text{m}^{-3}$	$\epsilon_r(T_n, P)$
$T_n = 303.15\text{ K}$											
302.85	16	1467.19	4.1496	1466.27	4.1433	293.21	16	1496.22	4.3635	1496.40	4.3648
302.85	15	1462.38	4.1348	1461.46	4.1285	293.30	15	1491.59	4.3494	1492.05	4.3527
302.85	14	1457.44	4.1204	1456.50	4.1141	293.21	14	1487.40	4.3353	1487.58	4.3366
302.85	13	1452.35	4.1022	1451.39	4.0958	293.21	13	1482.81	4.3191	1483.00	4.3204
302.84	12	1447.13	4.0857	1446.12	4.0791	293.21	12	1478.10	4.3034	1478.29	4.3048
302.85	11	1441.67	4.0692	1440.68	4.0628	293.19	11	1473.31	4.2886	1473.44	4.2895
302.96	10	1435.69	4.0486	1435.04	4.0446	293.18	10	1468.34	4.2716	1468.44	4.2723
302.98	9	1429.79	4.0294	1429.20	4.0258	293.17	9	1463.21	4.2554	1463.28	4.2559
302.93	8	1423.91	4.0110	1423.13	4.0062	293.17	8	1457.88	4.2381	1457.95	4.2385
302.91	7	1417.68	3.9919	1416.81	3.9868	293.16	7	1452.39	4.2197	1452.43	4.2199
302.90	6	1411.15	3.9715	1410.22	3.9661	293.16	6	1446.67	4.2018	1446.70	4.2020
302.89	5	1404.31	3.9506	1403.32	3.9450	293.16	5	1440.72	4.1815	1440.76	4.1817
302.90	4	1397.06	3.9276	1396.07	3.9222	293.15	4	1434.56	4.1628	1434.56	4.1628
302.91	3	1389.42	3.9040	1388.44	3.8988	293.14	3	1428.13	4.1421	1428.09	4.1419
302.91	2	1381.38	3.8793	1380.36	3.8740	293.14	2	1421.36	4.1210	1421.32	4.1208
302.92	1	1372.79	3.8527	1371.78	3.8477	293.14	1	1414.25	4.0971	1414.21	4.0968
$T_n = 283.15\text{ K}$											
283.32	16	1525.50	4.5951	1526.00	4.5992	273.26	16	1554.81	4.8448	1555.13	4.8476
283.31	15	1521.58	4.5818	1522.06	4.5857	273.26	15	1551.23	4.8325	1551.55	4.8353
283.31	14	1517.55	4.5675	1518.03	4.5714	273.25	14	1547.61	4.8194	1547.90	4.8220
283.31	13	1513.41	4.5531	1513.90	4.5570	273.25	13	1543.87	4.8056	1544.17	4.8082
283.30	12	1509.20	4.5383	1509.67	4.5419	273.25	12	1540.06	4.7915	1540.36	4.7941
283.30	11	1504.85	4.5242	1505.33	4.5279	273.24	11	1536.18	4.7775	1536.46	4.7799
283.30	10	1500.39	4.5085	1500.87	4.5121	273.24	10	1532.19	4.7629	1532.47	4.7653
283.31	9	1495.77	4.4934	1496.29	4.4974	273.24	9	1528.10	4.7486	1528.38	4.7510
283.29	8	1491.11	4.4772	1491.57	4.4807	273.24	8	1523.90	4.7330	1524.19	4.7354
283.29	7	1486.24	4.4605	1486.72	4.4640	273.23	7	1519.62	4.7171	1519.88	4.7192
283.30	6	1481.19	4.4424	1481.70	4.4461	273.23	6	1515.20	4.7014	1515.46	4.7035
283.29	5	1476.03	4.4246	1476.53	4.4280	273.23	5	1510.64	4.6859	1510.91	4.6880
283.29	4	1470.66	4.4064	1471.17	4.4099	273.23	4	1505.95	4.6687	1506.23	4.6708
283.29	3	1465.09	4.3874	1465.61	4.3909	273.23	3	1501.12	4.6514	1501.40	4.6536
283.28	2	1459.34	4.3692	1459.83	4.3724	273.23	2	1496.12	4.6243	1496.41	4.6264
283.28	1	1453.32	4.3488	1453.82	4.3521	273.33	1	1490.59	4.6147	1491.25	4.6196
$T_n = 263.15\text{ K}$											
262.70	16	1585.13	5.1264	1583.85	5.1139	253.85	16	1610.24	5.3768	1612.21	5.3978
262.78	15	1581.66	5.1145	1580.60	5.1042	253.71	15	1607.65	5.3683	1609.25	5.3852
262.84	14	1578.18	5.0998	1577.28	5.0911	253.59	14	1604.97	5.3603	1606.23	5.3735
262.91	13	1574.61	5.0849	1573.90	5.0781	253.51	13	1602.12	5.3514	1603.16	5.3623
262.96	12	1571.02	5.0701	1570.46	5.0647	253.37	12	1599.39	5.3426	1600.04	5.3493
263.04	11	1567.27	5.0518	1566.94	5.0487	253.30	11	1596.42	5.3323	1596.86	5.3369
263.06	10	1563.63	5.0388	1563.35	5.0363	253.26	10	1593.29	5.3213	1593.62	5.3247
263.10	9	1559.84	5.0228	1559.69	5.0214	253.19	9	1590.20	5.3100	1590.32	5.3112
263.11	8	1556.06	5.0093	1555.94	5.0082	253.17	8	1586.89	5.2979	1586.96	5.2985
263.12	7	1552.20	4.9942	1552.10	4.9933	253.14	7	1583.55	5.2848	1583.52	5.2845
263.13	6	1548.24	4.9801	1548.18	4.9796	253.13	6	1580.08	5.2721	1580.02	5.2715
263.13	5	1544.22	4.9640	1544.15	4.9634	253.12	5	1576.53	5.2584	1576.43	5.2574
263.14	4	1540.06	4.9485	1540.02	4.9482	253.11	4	1572.90	5.2439	1572.77	5.2427
263.15	3	1535.79	4.9316	1535.79	4.9316	253.10	3	1569.19	5.2301	1569.03	5.2286
263.16	2	1531.40	4.9147	1531.43	4.9150	253.09	2	1565.39	5.2150	1565.19	5.2131
263.17	1	1526.88	4.8983	1526.95	4.8988	253.08	1	1561.49	5.1993	1561.26	5.1971
$T_n = 243.15\text{ K}$											
243.65	16	1638.89	5.6960	1640.28	5.7122	233.27	16	1667.79	6.0505	1668.12	6.0547
243.66	15	1636.14	5.6842	1637.57	5.7009	233.27	15	1665.30	6.0407	1665.64	6.0449
243.65	14	1633.40	5.6731	1634.82	5.6894	233.27	14	1662.79	6.0290	1663.13	6.0333
243.65	13	1630.59	5.6622	1632.03	5.6786	233.27	13	1660.24	6.0185	1660.58	6.0227
243.65	12	1627.74	5.6494	1629.19	5.6658	233.27	12	1657.65	6.0081	1657.99	6.0124
243.65	11	1624.85	5.6376	1626.31	5.6542	233.27	11	1655.02	5.9957	1655.37	6.0001
243.65	10	1621.90	5.6248	1623.38	5.6414	233.27	10	1652.36	5.9845	1652.71	5.9888
243.64	9	1618.93	5.6127	1620.40	5.6290	233.26	9	1649.69	5.9716	1650.01	5.9756
243.65	8	1615.85	5.5990	1617.36	5.6157	233.27	8	1646.91	5.9598	1647.27	5.9641
243.65	7	1612.75	5.5865	1614.27	5.6032	233.26	7	1644.15	5.9463	1644.48	5.9503
243.65	6	1609.59	5.5742	1611.13	5.5910	233.26	6	1641.31	5.9336	1641.65	5.9376
243.65	5	1606.37	5.5604	1607.92	5.5773	233.26	5	1638.43	5.9217	1638.77	5.9257
243.64	4	1603.11	5.5465	1604.66	5.5631	233.26	4	1635.50	5.9093	1635.84	5.9133
243.64	3	1599.76	5.5324	1601.32	5.5491	233.26	3	1632.51	5.8971	1632.85	5.9012
243.64	2	1596.34	5.5192	1597.92	5.5359	233.26	2	1629.47	5.8828	1629.82	5.8869
243.63	1	1592.88	5.5056	1594.45	5.5220	233.26	1	1626.38	5.8696	1626.73	5.8736
$T_n = 223.15\text{ K}$											
223.05	16	1696.05	6.4357	1695.78	6.4318	223.03	8	1677.12	6.3530	1676.77	6.3483
223.05	15	1693.79	6.4283	1693.51	6.4245	223.03	7	1674.60	6.3422	1674.24	6.3375
223.05	14	1691.49	6.4191	1691.21	6.4152	223.03	6	1672.04	6.3306	1671.68	6.3258
223.05	13	1689.16	6.4093	1688.88	6.4054	223.03	5	1669.45	6.3186	1669.09	6.3138
223.05	12	1686.80	6.3981	1686.52	6.3942	223.03	4	1666.81	6.3073	1666.45	6.3025
223.04	11	1684.45	6.3856	1684.13	6.3813	223.03	3	1664.14	6.2941	1663.77	6.2893
223.05	10	1682.00	6.3748	1681.71	6.3708	223.02	2	1661.45	6.2819	1661.05	6.2767
223.04	9	1679.58	6.3640	1679.26	6.3597	223.02	1	1658.69	6.2689	1658.28	6.2637

**Table 3.** Relative Permittivity  $\epsilon_r$  of HFC-236ea, from  $T = 223.15\text{ K}$  to  $303.15\text{ K}$  and up to  $P = 16\text{ MPa}$ 

$T/\text{K}$	$P/\text{MPa}$	$\rho/\text{kg}\cdot\text{m}^{-3}$	$\epsilon_r(T, P)$	$\rho(T_n, P)/\text{kg}\cdot\text{m}^{-3}$	$\epsilon_r(T_n, P)$	$T/\text{K}$	$P/\text{MPa}$	$\rho/\text{kg}\cdot\text{m}^{-3}$	$\epsilon_r(T, P)$	$\rho(T_n, P)/\text{kg}\cdot\text{m}^{-3}$	$\epsilon_r(T_n, P)$
$T_n = 303.15\text{ K}$											
302.85	16	1470.02	5.3286	1469.23	5.3287	293.21	16	1495.09	5.6327	1495.25	5.6327
302.85	15	1466.79	5.3105	1465.99	5.3106	293.30	15	1491.88	5.6151	1492.27	5.6150
302.85	14	1463.49	5.2919	1462.69	5.2920	293.21	14	1489.09	5.5968	1489.25	5.5967
302.85	13	1460.13	5.2714	1459.31	5.2715	293.21	13	1486.01	5.5774	1486.17	5.5774
302.84	12	1456.72	5.2518	1455.87	5.2519	293.21	12	1482.87	5.5585	1483.03	5.5584
302.85	11	1453.18	5.2311	1452.35	5.2312	293.19	11	1479.72	5.5386	1479.83	5.5386
302.96	10	1449.28	5.2109	1448.75	5.2109	293.18	10	1476.48	5.5170	1476.57	5.5170
302.98	9	1445.55	5.1886	1445.06	5.1887	293.17	9	1473.18	5.4987	1473.23	5.4987
302.93	8	1441.92	5.1687	1441.29	5.1688	293.17	8	1469.77	5.4787	1469.83	5.4787
302.91	7	1438.12	5.1479	1437.42	5.1480	293.16	7	1466.32	5.4590	1466.35	5.4590
302.90	6	1434.19	5.1272	1433.45	5.1273	293.16	6	1462.76	5.4372	1462.79	5.4372
302.89	5	1430.16	5.1028	1429.38	5.1029	293.16	5	1459.12	5.4153	1459.15	5.4153
302.90	4	1425.95	5.0809	1425.19	5.0809	293.15	4	1455.42	5.3950	1455.42	5.3950
302.91	3	1421.62	5.0572	1420.87	5.0572	293.14	3	1451.63	5.3720	1451.59	5.3720
302.91	2	1417.20	5.0343	1416.43	5.0343	293.14	2	1447.70	5.3498	1447.67	5.3499
302.92	1	1412.59	5.0076	1411.85	5.0077	293.14	1	1443.67	5.3249	1443.64	5.3249
$T_n = 283.15\text{ K}$											
283.32	16	1520.56	5.9362	1520.99	5.9361	273.26	16	1546.27	6.2732	1546.54	6.2732
283.31	15	1517.85	5.9189	1518.26	5.9189	273.26	15	1543.75	6.2557	1544.03	6.2556
283.31	14	1515.07	5.8993	1515.49	5.8992	273.25	14	1541.22	6.2381	1541.48	6.2381
283.31	13	1512.25	5.8796	1512.67	5.8795	273.25	13	1538.63	6.2214	1538.89	6.2214
283.30	12	1509.40	5.8618	1509.80	5.8618	273.25	12	1535.99	6.2033	1536.26	6.2033
283.30	11	1506.48	5.8436	1506.88	5.8435	273.24	11	1533.35	6.1843	1533.58	6.1843
283.30	10	1503.50	5.8249	1503.91	5.8249	273.24	10	1530.63	6.1646	1530.87	6.1646
283.31	9	1500.44	5.8042	1500.88	5.8041	273.24	9	1527.86	6.1460	1528.11	6.1460
283.29	8	1497.41	5.7838	1497.79	5.7838	273.24	8	1525.05	6.1283	1525.30	6.1282
283.29	7	1494.26	5.7657	1494.65	5.7657	273.23	7	1522.22	6.1061	1522.44	6.1061
283.30	6	1491.02	5.7446	1491.44	5.7446	273.23	6	1519.31	6.0874	1519.53	6.0874
283.29	5	1487.76	5.7233	1488.17	5.7233	273.23	5	1516.35	6.0683	1516.57	6.0683
283.29	4	1484.41	5.7027	1484.82	5.7027	273.23	4	1513.33	6.0495	1513.56	6.0495
283.29	3	1480.99	5.6797	1481.40	5.6797	273.23	3	1510.25	6.0289	1510.48	6.0289
283.28	2	1477.52	5.6571	1477.91	5.6571	273.23	2	1507.12	6.0065	1507.35	6.0065
283.28	1	1473.94	5.6364	1474.33	5.6364	273.33	1	1503.62	5.9827	1504.15	5.9827
$T_n = 263.15\text{ K}$											
262.70	16	1573.12	6.6328	1571.97	6.6330	252.91	16	1599.20	7.0345	1598.42	7.0347
262.78	15	1570.60	6.6143	1569.65	6.6145	252.91	15	1596.78	7.0168	1596.01	7.0169
262.84	14	1568.10	6.5960	1567.30	6.5962	252.91	14	1594.36	7.0015	1593.61	7.0016
262.91	13	1565.54	6.5791	1564.91	6.5792	252.91	13	1591.94	6.9830	1590.83	6.9832
262.96	12	1562.99	6.5594	1562.49	6.5595	252.91	12	1589.22	6.9644	1588.60	6.9645
263.04	11	1560.33	6.5419	1560.04	6.5419	252.91	11	1586.97	6.9461	1586.34	6.9462
263.06	10	1557.79	6.5245	1557.55	6.5245	252.91	10	1584.68	6.9286	1584.05	6.9286
263.10	9	1555.16	6.5051	1555.02	6.5051	252.91	9	1582.37	6.9106	1581.73	6.9107
263.11	8	1552.56	6.4868	1552.46	6.4868	252.91	8	1580.02	6.8913	1579.37	6.8913
263.12	7	1549.93	6.4671	1549.85	6.4671	252.91	7	1577.64	6.8717	1576.99	6.8718
263.13	6	1547.26	6.4462	1547.20	6.4462	252.91	6	1575.22	6.8529	1574.57	6.8530
263.13	5	1544.57	6.4265	1544.51	6.4265	252.91	5	1572.77	6.8327	1572.11	6.8327
263.14	4	1541.81	6.4062	1541.78	6.4062	252.91	4	1570.29	6.8142	1569.62	6.8143
263.15	3	1539.00	6.3835	1539.00	6.3835	252.91	3	1567.76	6.7940	1567.09	6.7940
263.16	2	1536.14	6.3645	1536.17	6.3645	252.91	2	1565.20	6.7729	1564.52	6.7729
263.17	1	1533.23	6.3443	1533.29	6.3443	252.91	1	1562.60	6.7535	1561.92	6.7535
$T_n = 243.15\text{ K}$											
243.60	16	1622.00	7.4340	1622.29	7.4337	233.27	16	1653.93	7.8701	1654.22	7.9218
243.60	15	1620.00	7.4187	1620.30	7.4185	233.27	15	1650.93	7.8543	1651.23	7.8989
243.60	14	1617.01	7.3924	1617.28	7.3922	233.27	14	1648.93	7.8373	1649.21	7.8835
243.60	13	1614.01	7.3775	1614.29	7.3773	233.27	13	1646.93	7.8204	1647.21	7.8682
243.60	12	1612.02	7.3585	1612.30	7.3583	233.27	12	1644.93	7.8021	1645.22	7.8530
243.60	11	1610.02	7.3379	1610.27	7.3377	233.27	11	1642.93	7.7826	1643.18	7.8375
243.60	10	1607.03	7.3184	1607.28	7.3182	233.27	10	1639.93	7.7649	1640.19	7.8146
243.60	9	1604.03	7.3014	1604.29	7.3012	233.26	9	1638.73	7.7448	1639.00	7.8055
243.60	8	1602.04	7.2827	1602.29	7.2826	233.27	8	1634.93	7.7271	1635.19	7.7765
243.60	7	1600.04	7.2611	1600.27	7.2609	233.26	7	1634.24	7.7079	1634.47	7.7710
243.60	6	1598.04	7.2472	1598.27	7.2471	233.26	6	1631.90	7.6876	1632.14	7.7532
243.60	5	1595.05	7.2305	1595.28	7.2304	233.26	5	1629.75	7.6720	1629.99	7.7368
243.60	4	1592.05	7.2089	1592.30	7.2088	233.26	4	1628.16	7.6530	1628.41	7.7247
243.60	3	1590.06	7.1900	1590.30	7.1900	233.26	3	1626.52	7.6328	1626.77	7.7121
243.60	2	1588.06	7.1577	1588.31	7.1577	233.26	2	1623.68	7.6138	1623.93	7.6905
243.60	1	1588.93	7.1496	1589.49	7.1495	233.26	1	1622.00	7.5923	1622.57	7.6801
$T_n = 223.15\text{ K}$											
223.05	16	1681.55	8.4810	1680.73	8.4159	223.03	8	1665.85	8.3348	1665.17	8.2924
223.05	15	1679.84	8.4644	1679.04	8.4025	223.03	7	1664.18	8.3163	1663.50	8.2791
223.05	14	1678.12	8.4459	1677.32	8.3889	223.03	6	1662.45	8.2980	1661.76	8.2654
223.05	13	1675.44	8.4292	1674.27	8.3647	223.03	5	1660.79	8.2788	1660.09	8.2521
223.05	12	1673.66	8.4116	1673.00	8.3546	223.03	4	1659.17	8.2595	1658.47	8.2392
223.04	11	1672.00	8.3926	1671.34	8.3414	223.03	3	1656.78	8.2387	1656.07	8.2202
223.05	10	1669.93	8.3745	1669.26	8.3249	223.02	2	1654.07	8.2188	1653.35	8.1986
223.04	9	1668.00	8.3552	1667.33	8.3096	223.02	1	1652.40	8.1984	1651.68	8.1854

**Table 4.** Relative Permittivity,  $\epsilon$ , of HFC-365mfc, from  $T = 263.15\text{ K}$  to  $303.15\text{ K}$  and up to  $P = 16\text{ MPa}$ 

$T/\text{K}$	$P/\text{MPa}$	$\rho/\text{kg}\cdot\text{m}^{-3}$	$\epsilon_r(T, P)$	$\rho(T_n, P)/\text{kg}\cdot\text{m}^{-3}$	$\epsilon_r(T_n, P)$	$T/\text{K}$	$P/\text{MPa}$	$\rho/\text{kg}\cdot\text{m}^{-3}$	$\epsilon_r(T, P)$	$\rho(T_n, P)/\text{kg}\cdot\text{m}^{-3}$	$\epsilon(T_n, P)$
$T_n = 303.15\text{ K}$											
303.01	16	1286.15	11.7786	1285.89	11.7676	293.23	16	1304.11	12.5349	1304.25	12.5416
303.01	15	1284.16	11.7450	1283.90	11.7340	293.23	15	1302.26	12.5018	1302.41	12.5085
303.01	14	1282.14	11.7115	1281.88	11.7004	293.23	14	1300.40	12.4690	1300.55	12.4757
303.01	13	1280.09	11.6764	1279.83	11.6654	293.23	13	1298.50	12.4364	1298.65	12.4432
303.01	12	1278.01	11.6429	1277.74	11.6318	293.23	12	1296.58	12.4025	1296.73	12.4092
303.01	11	1275.88	11.6078	1275.61	11.5968	293.23	11	1294.62	12.3672	1294.78	12.3740
303.01	10	1273.73	11.5749	1273.45	11.5638	293.23	10	1292.64	12.3321	1292.79	12.3389
303.01	9	1271.53	11.5382	1271.25	11.5271	293.23	9	1290.62	12.2974	1290.78	12.3042
303.01	8	1269.29	11.5028	1269.01	11.4916	293.23	8	1288.57	12.2608	1288.72	12.2676
303.01	7	1267.01	11.4659	1266.73	11.4547	293.23	7	1286.48	12.2260	1286.64	12.2328
303.00	6	1264.71	11.4290	1264.41	11.4170	293.22	6	1284.38	12.1866	1284.52	12.1926
303.00	5	1262.34	11.3908	1262.03	11.3788	293.22	5	1282.21	12.1498	1282.35	12.1557
303.00	4	1259.92	11.3535	1259.61	11.3415	293.23	4	1279.99	12.1135	1280.15	12.1203
303.00	3	1257.45	11.3146	1257.13	11.3026	293.23	3	1277.74	12.0713	1277.91	12.0781
303.00	2	1254.92	11.2750	1254.60	11.2630	293.23	2	1275.45	12.0329	1275.62	12.0397
303.00	1	1252.34	11.2337	1252.02	11.2217	293.23	1	1273.11	11.9936	1273.28	12.0005
$T_n = 283.15\text{ K}$											
283.11	16	1322.59	13.4493	1322.51	13.4457	273.20	16	1340.62	14.3733	1340.71	14.3781
283.11	15	1320.88	13.4183	1320.81	13.4147	273.19	15	1339.06	14.3437	1339.13	14.3476
283.12	14	1319.14	13.3889	1319.09	13.3862	273.19	14	1337.46	14.3131	1337.53	14.3170
283.11	13	1317.41	13.3541	1317.34	13.3505	273.19	13	1335.84	14.2819	1335.92	14.2858
283.11	12	1315.64	13.3213	1315.56	13.3177	273.19	12	1334.20	14.2520	1334.28	14.2559
283.11	11	1313.84	13.2847	1313.76	13.2810	273.19	11	1332.54	14.2212	1332.62	14.2251
283.10	10	1312.03	13.2519	1311.94	13.2473	273.19	10	1330.86	14.1868	1330.94	14.1907
283.10	9	1310.18	13.2072	1310.08	13.2026	273.19	9	1329.15	14.1510	1329.23	14.1549
283.11	8	1308.28	13.1743	1308.20	13.1707	273.18	8	1327.44	14.1193	1327.50	14.1223
283.11	7	1306.37	13.1372	1306.29	13.1336	273.18	7	1325.69	14.0864	1325.74	14.0894
283.11	6	1304.43	13.1003	1304.35	13.0967	273.19	6	1323.89	14.0488	1323.96	14.0527
283.10	5	1302.47	13.0635	1302.38	13.0590	273.18	5	1322.10	14.0155	1322.16	14.0185
283.10	4	1300.47	13.0232	1300.37	13.0186	273.18	4	1320.26	13.9789	1320.32	13.9819
283.11	3	1298.41	12.9815	1298.33	12.9779	273.18	3	1318.40	13.9444	1318.46	13.9473
283.10	2	1296.35	12.9424	1296.25	12.9379	273.18	2	1316.50	13.9070	1316.56	13.9099
283.10	1	1294.23	12.8983	1294.13	12.8937	273.18	1	1314.58	13.8707	1314.64	13.8736
$T_n = 263.15\text{ K}$											
263.16	16	1358.85	15.3760	1358.87	15.3771	263.15	8	1346.66	15.1352	1346.66	15.1352
263.15	15	1357.41	15.3453	1357.41	15.3453	263.15	7	1345.05	15.0997	1345.05	15.0997
263.15	14	1355.93	15.3179	1355.93	15.3179	263.15	6	1343.41	15.0681	1343.41	15.0681
263.15	13	1354.43	15.2925	1354.43	15.2925	263.14	5	1341.77	15.0355	1341.75	15.0344
263.14	12	1352.93	15.2606	1352.92	15.2595	263.15	4	1340.07	15.0010	1340.07	15.0010
263.14	11	1351.40	15.2295	1351.38	15.2284	263.14	3	1338.39	14.9675	1338.37	14.9664
263.15	10	1349.83	15.1979	1349.83	15.1979	263.14	2	1336.66	14.9339	1336.64	14.9328
263.14	9	1348.28	15.1666	1348.26	15.1655	263.14	1	1334.90	14.8991	1334.88	14.8980

(iterations implemented by a Levenberg–Marquardt procedure), of the following form ( $T$  in K and  $\rho$  in  $\text{kg}\cdot\text{m}^{-3}$ )

$$\epsilon_r(\rho, T) = \frac{a_1}{T} + a_2\rho + \frac{a_3\rho}{T} \quad (2)$$

with a standard deviation of 0.15 % for HFC-227ea (number of points = 143,  $r = 0.99992$ ), 0.034 % for HFC-236ea (number of points = 143,  $r = 0.99946$ ), and 0.12 % for HFC-365mfc (number of points = 79,  $r = 0.99992$ ). For industrial use the data were also fitted to a function in pressure and temperature according to the equation ( $P$  in MPa and  $T$  in K)

$$\epsilon_r(P, T) = b_0 + \frac{b_1}{T} + b_2P + \frac{b_3P}{T} \quad (3)$$

with a standard deviation of 0.11 % for HFC-227ea (number of points = 143,  $r = 0.99996$ ), 0.023 % for HFC-236ea (number of points = 143,  $r = 0.99974$ ), and 0.017 % for HFC-365mfc (number of points = 79,  $r = 0.99992$ ). The coefficients of eqs 2 and 3, together with their uncertainty, are given in Table 5.

The relative permittivity data can be analyzed using the Vedam formalism.<sup>16–18</sup> According to this theory, the variation of the relative permittivity with pressure is a function of the deformation of volume, showing a nonlinear behavior in the case of the liquids. This nonlinearity can be reduced when the

variation of  $\epsilon_r$ ,  $\Delta$ , is analyzed as a function of the Eulerian deformation,  $\Sigma$ , also named the Eulerian strain. It has been demonstrated before that  $\Sigma$  provides a linear relation for  $\Delta$  independently of the type of molecules that compose the fluid. According to Vedam,<sup>16,17</sup> the relationship between  $\epsilon_r^{1/2}$  and the Eulerian strain,  $\Sigma$ , is linear:

$$\Delta = \epsilon_r^{1/2}(\rho) - \epsilon_r^{1/2}(\rho_0) = A\Sigma + B \quad (4)$$

$$\Sigma = \frac{1}{2} \left[ \left( 1 - \frac{\rho}{\rho_0} \right)^{2/3} \right] \quad (5)$$

In eqs 4 and 5  $\rho_0$  is the reference density, chosen as the liquid saturation density for each isotherm. The value of  $\epsilon_r(\rho_0)$  was calculated from eq 2. Calculations show that the function  $\Delta$  varies linearly with the Eulerian strain,  $\Sigma$ , as shown for HFC-227ea, HFC-236ea, and HFC-365mfc in Figure 5, except for HFC-227ea at the higher densities. This behavior has not been found with other refrigerants and can be possibly attributed to minor deviations of the linear Vedam model for this refrigerant. Table 6 presents the values of the coefficients  $A$  and  $B$  of the Vedam equation for each isotherm of the three refrigerants. The behavior found for these refrigerants is similar to all studied before.<sup>14</sup> The intercept values are nearly zero for all isotherms,  $B \approx 0$ , and the slope of the linear variation of  $\Delta$  with  $\Sigma$  is

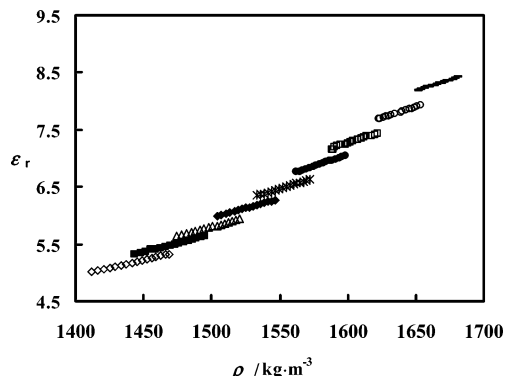


**Figure 2.** Relative permittivity,  $\epsilon_r$ , of HFC-227ea as a function of density,  $\rho$ , at nominal temperatures:  $\diamond$ , 303.15 K;  $\blacksquare$ , 293.15 K;  $\triangle$ , 283.15 K;  $\blacklozenge$ , 273.15 K;  $*$ , 263.15 K;  $\bullet$ , 253.15 K;  $\square$ , 243.15 K;  $\circ$ , 233.15 K; —, 223.15 K.

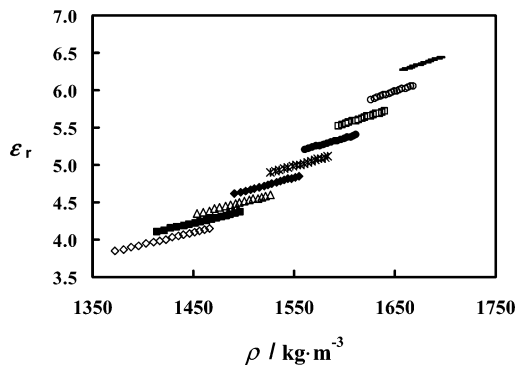


**Figure 3.** Relative permittivity,  $\epsilon_r$ , of HFC-236ea as a function of density,  $\rho$ , at nominal temperatures:  $\diamond$ , 303.15 K;  $\blacksquare$ , 293.15 K;  $\triangle$ , 283.15 K;  $\blacklozenge$ , 273.15 K;  $*$ , 263.15 K;  $\bullet$ , 253.15 K;  $\square$ , 243.15 K;  $\circ$ , 233.15 K; —, 223.15 K.

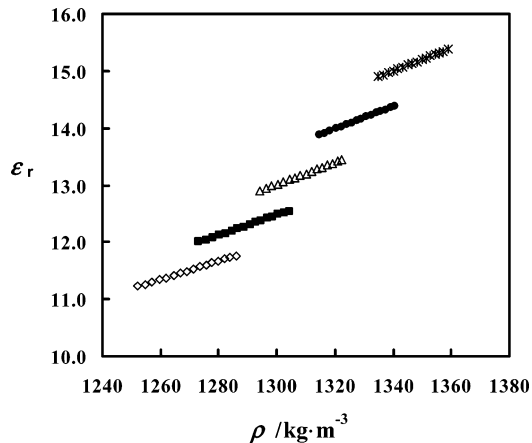


**Figure 4.** Relative permittivity,  $\epsilon_r$ , of HFC-236ea as a function of density,  $\rho$ , at nominal temperatures:  $\diamond$ , 303.15 K;  $\blacksquare$ , 293.15 K;  $\triangle$ , 283.15 K;  $\blacklozenge$ , 273.15 K;  $*$ , 263.15 K.

negative for all temperatures, decreasing linearly with the increase with temperature, as expected from the theory. Assuming that  $B = 0$  (eq 4), it is possible to use the Vedam relationship to estimate the relative permittivity values. As reported before, the values for  $A'$  were estimated by fitting the experimental data as a function of  $\Sigma$  and forcing the constant  $B$

**Table 6.** Values of Constants  $A$  and  $B$  of the Vedam Equation and  $A'$  in Equations 4 and 6

refrigerant	$T$ K	$\rho_0$ $\text{kg}\cdot\text{m}^{-3}$	$\epsilon_r(\rho_0)$	Equation 4		
				$A$	$B$	$A'$
HFC-227ea	303.15	1367.52	3.8229	-3.2611	0.00269	-3.4186
	293.15	1409.67	4.0759	-3.3939	0.00144	-3.4935
	283.15	1449.33	4.3375	-3.5585	-0.00038	-3.5280
	273.15	1486.96	4.6104	-3.7684	-0.00246	-3.5391
	263.15	1522.95	4.8973	-3.9227	-0.00325	-3.5747
	253.15	1557.58	5.2010	-4.0009	-0.00385	-3.5304
	243.15	1591.09	5.5244	-4.2228	-0.00367	-3.7121
	233.15	1623.68	5.8711	-4.4165	-0.00229	-4.0558
	223.15	1655.52	6.2448	-4.4952	0.00147	-4.7555
HFC-236ea	303.15	1408.28	4.9606	-5.2298	0.00591	-5.8135
	293.15	1440.22	5.2840	-5.5293	0.00442	-6.0254
	283.15	1471.11	5.6212	-5.9334	-0.00142	-5.7532
	273.15	1501.14	5.9752	-6.2288	-0.00232	-5.8983
	263.15	1530.50	6.3493	-6.7638	-0.00533	-5.9172
	253.15	1559.35	6.7471	-6.9781	-0.00239	-6.5605
	243.15	1590.72	7.1939	-7.0859	-0.00166	-6.7297
	233.15	1620.90	7.6673	-6.6714	0.00004	-6.6800
	223.15	1651.08	8.1806	-6.8414	0.00003	-6.8486
HFC-365mfc	303.15	1250.55	11.1533	-8.9397	0.00648	-9.9253
	293.15	1271.87	11.9923	-9.5762	-0.00259	-9.1449
	283.15	1292.78	12.8861	-10.4697	-0.00214	-10.0768
	273.15	1313.36	13.8420	-10.2170	0.00089	-10.3983
	263.15	1333.66	14.8681	-10.3248	0.00072	-10.4873

to be equal to zero. That being the case, the Vedam equation takes the following form:

$$\Delta = A'\Sigma \quad (6)$$

The new values of the slope  $A'$  according to the eq 6 are also presented in Table 6. Values in Table 6 can be used to estimate the relative permittivity at any density for each temperature.

The only molecular theory that can be applied to the present data, in the absence of data on the refractive index of the liquid, is the theory of molecular polarizability developed by Kirkwood after the definition of Onsager's local field.<sup>19,20</sup> In this theory, an apparent dipole moment of the liquid  $\mu^*$  is calculated from the Kirkwood function (KF)

$$KF = \frac{(\epsilon_r - 1)(2\epsilon_r + 1)}{9\epsilon_r} \left( \frac{M}{\rho} \right) = \frac{N_A}{3} \left( \alpha + \frac{g\mu^2}{3\epsilon_0 k_B T} \right) \quad (7)$$

where  $M$  is the relative molar mass of the fluid,  $N_A$  is the Avogadro constant,  $\alpha$  is the molecular polarizability of the molecule,  $\epsilon_0$  is the electric permittivity in a vacuum,  $T$  is the absolute temperature,  $k_B$  is the Boltzmann constant, and  $\rho$  is the density. The apparent dipole moment is defined as  $\mu^* = g^{1/2}\mu$ , where  $\mu$  is the dipole moment in the ideal gas state and  $g$  is the Kirkwood correlation parameter, which measures the restriction to rotation imposed by a cage of molecules surrounding a given one. Kirkwood,<sup>19</sup> on the basis of a quasi-crystalline model, defined this parameter  $g$  as

$$g = \frac{\mu^{*2}}{\mu^2} = 1 + \sum_{i=1}^{\infty} z_i \langle \cos \gamma_i \rangle \quad (8)$$

where  $z_i$  is the number of neighbors to the central molecule under consideration in the  $i$ th coordination shell and  $\langle \cos \gamma_i \rangle$  is the average cosine angle  $\gamma$  formed by the dipole moments of

**Table 5.** Coefficients of the Dielectric Equations of State (Equations 2 and 3)

refrigerant	$a_1/K$	$10^{-3}a_2/\text{kg}^{-1}\cdot\text{m}^3$	$a_3/\text{K}\cdot\text{m}^3\cdot\text{kg}^{-1}$	$b_0$	$b_1/K$	$10^{-2}b_2/\text{MPa}^{-1}$	$b_3/\text{K}\cdot\text{MPa}^{-1}$
HFC-227ea	$-145.94 \pm 16.075$	$-0.3033 \pm 0.0215$	$0.8622 \pm 0.0051$	$-2.8306 \pm 0.0125$	$2028.9 \pm 3.2303$	$4.0490 \pm 0.1310$	$-6.6918 \pm 0.3384$
HFC-236ea	$-1097.95 \pm 91.19$	$0.9605 \pm 0.1062$	$1.556 \pm 0.032$	$-3.7473 \pm 0.042$	$2652.2 \pm 10.852$	$26.718 \pm 4.393$	$-1.9026 \pm 1.137$
HFC-365mfc	$-3041.7 \pm 80.268$	$-1.96 \pm 0.0960$	$5.73 \pm 0.036$	$-13.144 \pm 0.079$	$7370.8 \pm 22.287$	$6.5717 \pm 0.8373$	$-8.6918 \pm 2.3563$

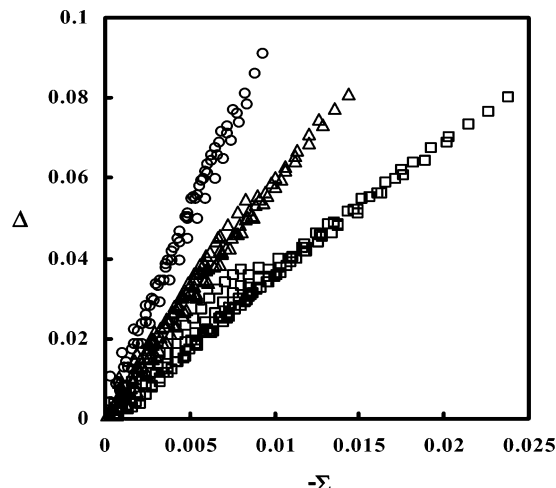


**Figure 5.** Function Delta ( $\Delta$ ) as a function of the Eulerian strain ( $\Sigma$ ) for □, HFC-227ea; △, HFC-236ea; and ○, HFC-365mfc.

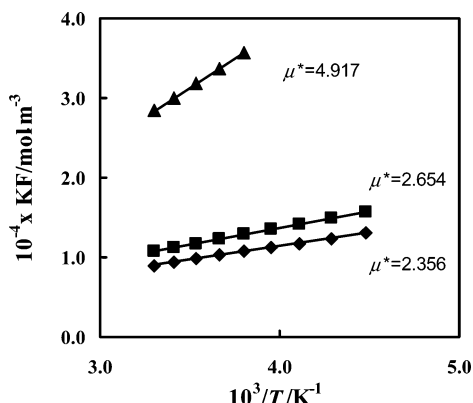


**Figure 6.** Kirkwood function as a function of  $1/T$  for ◆, HFC-227ea; ■, HFC-236ea; and ▲, HFC-365mfc; —, Kirkwood fit.

**Table 7. Dipole Moments and Kirkwood Correlation Factors for HFC-227ea, HFC-236ea, and HFC-365mfc**

refrigerant	$\mu^*/\text{K}/\text{D}$	$\mu/\text{D}$	$g$
HFC-227ea	2.356	1.456	2.619
HFC-236ea	2.624	1.129	5.403
HFC-365mfc	4.917	3.790	1.683

molecules in the  $i$ th shell with the dipole of the central molecule. For nonpolar or nonassociated liquids  $g \approx 1$ , but for polar liquids it considerably differs from unity (for water, a value of 2.6 for  $z_i = 4$  was found). The greater the value of  $g$ , the bigger the orientational order imposed by the neighbors. If the theory is correct, the value of  $\mu^*$  can be calculated by a linear regression of the left-hand side of eq 7 as a function of  $1/T$ . The experimental measurements were used to calculate the Kirkwood function, and Figure 6 shows its variation with  $1/T$  for HFC-227ea, HFC-236ea, and HFC-365mfc. Table 7 displays the values obtained for the apparent dipole moments in the liquid phase, and using the values of the dipole moments in the gas phase,<sup>25</sup> the values of the Kirkwood parameter  $g$  were found to be equal to 2.619 for HFC-227ea, 5.403 for HFC-236ea, and 1.683 for HFC-365mfc.

## Discussion

In Figure 7 we compare our results with those obtained for HFC-236ea by Tanaka et al.,<sup>8</sup> the only refrigerant for which data were available, and for the highest temperatures, 293.15 K and 303.15 K. The departures between the two sets of data are of the order of 2 %, and the discrepancy can be

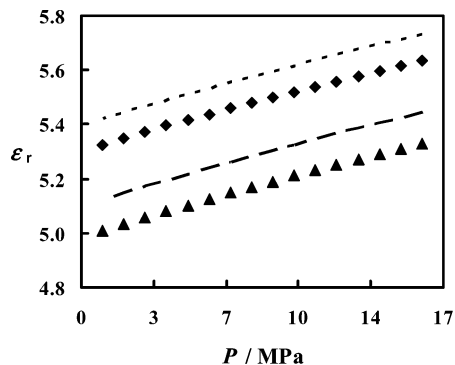


**Figure 7.** Comparison between our values and Tanaka et al.'s:<sup>8</sup> - - -, 293.15 K, ref 8; —, 303.15 K, ref 8; ♦, 293.15 K, present work; ▲, 303.15 K, present work.

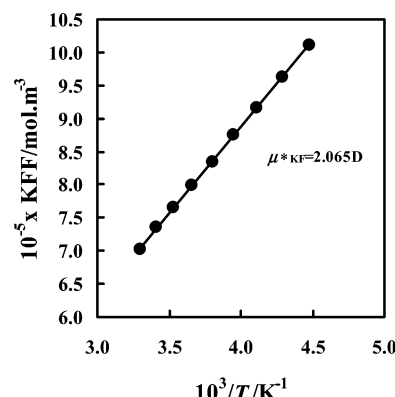


**Figure 8.** Kirkwood-Frölich function versus  $1/T$  for HFC-236ea; —, Kirkwood-Frölich fit.

justified by the presence of water as an impurity in the previous study (700 ppm of water justifies the difference in the permittivity).<sup>27</sup>

Experimental measurements of dielectric permittivity have raised issues regarding liquid-phase structure of ethane- and propane-based alternative refrigerants. Theoretical studies are performed to provide insight into the phenomena. In the liquid phase the molecules are close to each other, so the orientation polarization of a molecule is influenced by the surrounding electric cavity. Onsager has given a more careful treatment of the continuum approach. In his model, a point dipole is placed in the center of a cavity of relative permittivity  $\epsilon_{r,\infty}$ , and the effect of the surrounding electric cavity is measured by the dielectric response of the polarization charges induced on the wall of the cavity, resulting in

$$\frac{(\epsilon_r - \epsilon_{r,\infty})(2\epsilon_r + \epsilon_{r,\infty})}{\epsilon_r(\epsilon_{r,\infty} + 2)^2} \left( \frac{M}{\rho} \right) = \frac{N_A g \mu^2}{9\epsilon_0 k_B T} \quad (9)$$

$$\text{KFF} = \frac{(\epsilon_r - n^2)(2\epsilon_r + n^2)}{\epsilon_r(n^2 + 2)^2} \left( \frac{M}{\rho} \right) = \frac{N_A g \mu^2}{9\epsilon_0 k_B T} \quad (10)$$

The high-frequency relative permittivity,  $\epsilon_{r,\infty}$ , is commonly calculated from the Maxwell relationship,  $\epsilon_{r,\infty} = n^2$ , where  $n$  is the refractive index of the liquid at temperature  $T$ . Equation 9 is then transformed in the Kirkwood-Frölich equation,<sup>21</sup> eq 10, where KFF is the Kirkwood-Frölich function. This equation was used to predict the apparent dipole in the liquid state of HFC-236ea ( $\mu^*_{\text{KF}} = 2.065 \text{ D}$ ). The Kirkwood-Frölich parameter,  $g$ , is 3.348. Figure 8 shows the experimental measurements and its variation with  $1/T$  for HFC-236ea.

Looking to the values obtained for the apparent dipole moments in the liquid phase, the corresponding values for the

**Table 8. Comparison between Theoretical (SCIPCM) and Experimental Values for HFC-227ea**

	theoretical	experimental
$\mu$ [B3LYP/d95V(d,p)]	1.237	1.456
$\mu^*_K (\epsilon)$ [B3LYP/cc-pVDZ]	1.977	2.356

dipole moments in the gaseous phase, and the Kirkwood factors, it was found that the HFCs and the HCFCs exhibit gas-phase dipole moments ( $\mu$ ) in the following order: 236ea < 123 < 227ea < 245fa < 125 < 134a < 32 < 141b < 142b < 152a < 143a < 365mfc. The values obtained for the liquid phase ( $\mu^*$ ), based on the Kirkwood theory, have a slightly different trend given by 123 < 227ea < 125 < 236ea < 245fa < 141b < 142b < 143a < 134a < 32 < 152a < 365mfc. As a consequence of these differences, the Kirkwood correlation factor,  $g$ , has an interesting behavior: 365 mfc < 143a < 141b < 142b < 123 < 125 < 227ea < 152a < 245fa < 32 < 134a < 236ea. We can see by the value of  $g$  for the HFC-365mfc that it possesses the higher mobility in the liquid phase. The reason for this is probably due to a structural rearrangement in the liquid phase caused by the proximity of other molecules. Therefore, the area of the molecule in the gas phase is larger than that in the liquid phase, making the rotation easier in the liquid phase.

The effective dipole in the liquid state of HFC-236ea ( $\mu^*_{KF}$ ) predicted by the Kirkwood–Frölich equation is 2.065 D, a value smaller than that obtained using Kirkwood theory ( $\mu^*_K = 2.619$  D).

Continuing the theoretical calculations presented before for other refrigerants,<sup>14,15</sup> the same approach was applied to HFC-227ea, on the basis of density functional theory. Details of the application can be found in the previous studies. This theory is dependent on the specific representation of the exchange correlation functional, and to represent exchange we have carried out calculations with Becke's three-parameter hybrid method for exchange (B3); correlation has been included by using the Lee, Yang, and Parr nonlocal functional (LYP). The basis sets used were the Dunning–Huzinaga valence double- $\xi$  [D95V-(d,p)] and the Dunning correlation consistent basis sets.

The dipole moment in the liquid phase for HFC-227ea calculated by the SCIPCM model is 1.98 D, a value that has to be compared with the Kirkwood value, 2.356 D (Table 8). The difference between the predicted and experimental values shows that the condensed phase predictions capture the qualitative behavior, but the numerical predictions are off, exhibiting the inability of the SCRF models to capture totally the condensed phase behavior, using a continuous medium. Our DFT results show that the large dipole moments of HFCs based on relative permittivity measurements and Kirkwood theory cannot be fully explained by polarization effects induced by hydrogen bonding. Reasons for this discrepancy are probably related to limitations of the Kirkwood theory and to the eventual formation in the liquid phase of dimers and small clusters in all of the liquids studied, carrying large dipoles, as mentioned previously.<sup>15</sup>

## Conclusions

This paper reports relative permittivity measurements for three alternative refrigerants, in wide temperature and pressure ranges in the liquid phase, the zone necessary for air-conditioning and refrigeration applications. The uncertainty of the measurements is estimated to be better than  $\pm 1.1 \cdot 10^{-2}$ . The experimental values were correlated as a function of density and temperature, generating two different dielectric equations of state for the three fluids. The Eulerian formalism was applied to analyze the data for the three refrigerants, and it was concluded that it represents

a successful estimation method for the dependence of the relative permittivity with density. Kirkwood theory allows a direct determination of the value of the apparent dipole moment,  $\mu^*$ , in the liquid phase, found to be 2.356 D for HFC-227ea, 2.624 D for HFC-236ea, and 4.917 D for HFC-365mfc, as well as the Kirkwood correlation factor,  $g$ , found to be 2.619 for HFC-227ea, 5.403 for HFC-236ea, and 1.683 for HFC-365mfc. Application of the more reliable Kirkwood–Frölich theory for the only refrigerant for which the refractive index is known, HFC-236ea, gives a value of 2.065 D, smaller, as expected, than the Kirkwood value.

The SCIPCM model was applied to HFC-227ea in the liquid phase, generating a value of 1.98 D, smaller than the Kirkwood value, 2.356 D. Reasons for this discrepancy are probably related to limitations of the Kirkwood theory and to the eventual formation in the liquid phase of dimers and small clusters in all of the liquids studied, carrying large dipoles, as reported before.

## Acknowledgment

We thank the following companies for delivery of the high-purity samples of the refrigerants: Ausimont S.p.A., Italy; Lancaster Inc., USA; and Solvay Fluor und Derivate, GmbH, Germany. We also thank Professor B. Cabral (Faculdade de Ciências da Universidade de Lisboa, Portugal) for having supervised the density functional theory and SCRF calculations for HFC-227ea.

## Literature Cited

- (1) Shi, L.; Duan, Y. Y.; Zhu, M. S.; Han, L. Z.; Lei, X. Gaseous Pressure–Volume–Temperature Properties of 1,1,1,2,3,3,3-Heptafluoropropane. *J. Chem. Eng. Data* **1999**, *44*, 1402–1408.
- (2) Liu, X. J.; Shi, L.; Han, L. Z.; Zhu, M. S. Liquid Viscosity of 1,1,1,2,3,3,3-Heptafluoropropane (HFC-227ea) along the Saturation Line. *J. Chem. Eng. Data* **1999**, *44*, 688–692.
- (3) Pátek, J.; Klomfar, J.; Prazák, J.; Sifner, O. The ( $p, \rho, T$ ) behaviour of 1,1,1,2,3,3,3-heptafluoropropane (HFC-227ea) measured with a Burnett apparatus. *J. Chem. Thermodyn.* **1998**, *30*, 1159–1172.
- (4) Liu, X. J.; Shi, L.; Duan, Y. Y.; Han, L. Z.; Zhu, M. S. Thermal Conductivity of Gaseous 1,1,1,2,3,3,3-Heptafluoropropane (HFC-227ea). *J. Chem. Eng. Data* **1999**, *44*, 882–886.
- (5) Defibaugh, D. R.; Gillis, K. A.; Moldover, M. R.; Schmidt, J. W.; Weber, L. A. Thermodynamic properties of  $\text{CF}_3\text{—CHF—CHF}_2$ , 1,1,1,2,3,3-hexafluoropropane. *Fluid Phase Equilib.* **1996**, *122*, 131–155.
- (6) Pires, P. F.; Esperança, J. M. S. S.; Guedes, J. R. Ultrasonic Speed of Sound and Derived Thermodynamic Properties of Liquid 1,1,1,2,3,3,3-Heptafluoropropane (HFC227ea) from 248 K to 333 K and Pressures up to 65 MPa. *J. Chem. Eng. Data* **2000**, *45*, 496–501.
- (7) Shi, L.; Duan, Y. Y.; Zhu, M. S.; Han, L. Z.; Lei, X. Vapor pressure of 1,1,1,2,3,3,3-heptafluoropropane. *Fluid Phase Equilib.* **1999**, *163*, 109–117.
- (8) Tanaka, Y.; Matsuo, S.; Yamada, M.; Matsuo, T.; Sotani, T. Relative permittivity of liquid HFC-236ea and HFC-245fa at temperatures from 293 to 343 K and pressures up to 50 MPa. *Fluid Phase Equilib.* **2000**, *170*, 127–138.
- (9) Cabaço, M. I.; Danten, Y.; Besnard, M.; Guissani, Y.; Guillot, B. Structural studies of liquid cyclopropane: from room temperature up to supercritical conditions. *Mol. Phys.* **1997**, *90*, 829–840.
- (10) Nicola, G. D.; Giuliani, G. Vapor Pressure and P–V–T Measurements for 1,1,1,2,3,3-Hexafluoropropane (R-236ea). *J. Chem. Eng. Data* **2000**, *45*, 1075–1079.
- (11) Laesecke, A.; Defibaugh, D. R. Viscosity of 1,1,1,2,3,3-Hexafluoropropane and 1,1,1,3,3,3-Hexafluoropropane at Saturated-Liquid Conditions from 262 K to 353 K. *J. Chem. Eng. Data* **1996**, *41*, 59–62.
- (12) Bobo, S.; Scatolini, M.; Fedele, L.; Camporese, R. Compressed liquid densities and saturated liquid densities of 365mfc. *Fluid Phase Equilib.* **2004**, *222–223*, 291–296.
- (13) Heinemann, T.; Klaen, W.; Yourd, R.; Dohrn, R. Experimental Determination of the Vapor Phase Thermal Conductivity of Blowing Agents for Polyurethane Rigid Foam. *J. Cell. Plast.* **2000**, *36*, 45–56.
- (14) Santos, F. J. V.; Pai-Panandiker, R. S.; Nieto de Castro, C. A.; Mardolcar, U. V. Dielectric Properties of Alternative Refrigerants. *IEEE Trans. Dielectr. Electr. Insul.* **2006**, *13*, 503–511.

- (15) Costa Cabral, B. J.; Guedes, R. C.; Pai-Panandiker, R. S.; Nieto de Castro, C. A. Hydrogen Bonding and Internal Rotation of Hydrofluorocarbons by Density Functional Theory. *Phys. Chem. Chem. Phys.* **2001**, *3*, 4200–4207.
- (16) Vedam, K. *CRC Crit. Rev. Solid Mater. Sci.* **1983**, *11*, 1–17.
- (17) Vedam, K.; Chen, C. Importance of using Eulerian representation of strain in high-pressure studies on liquids. *J. Chem. Phys.* **1982**, *77*, 1461–1463.
- (18) Diguet, R. Density Dependence of Refractive Index and Static Relative Permittivity. *Physica* **1986** *139–140B*, 126–130.
- (19) Kirkwood, J. G. The Dielectric Polarization of Polar Liquids. *J. Chem. Phys.* **1939**, *7*, 911–919.
- (20) Onsager, L. Electric moments of molecules in liquids. *J. Am. Chem. Soc.* **1936**, *58*, 1486–1491.
- (21) Frölich, H. *Theory of Dielectrics*; Oxford University Press: Oxford, U.K., 1958.
- (22) Mardolcar, U. V.; Nieto de Castro, C. A.; Santos, F. J. Relative Permittivity of Toluene and Benzene. *Fluid Phase Equilib.* **1992**, *79*, 255–264.
- (23) Pereira, L. M.; Brito, F. E.; Gurova, A. N.; Mardolcar, U. V.; Nieto de Castro, C. A. Dielectric Properties of Liquid Pentafluoropentane (HFC-125). *Int. J. Thermophys.* **2001**, *22*, 887–899.
- (24) Gurova, A. N.; Brito, F. E.; Mardolcar, U. V.; Nieto de Castro, C. A. Dielectric Properties of 1,1,1,3,3-Pentafluoropropane (HFC-245fa). *J. Chem. Eng. Data* **2001**, *46*, 1072–1077.
- (25) McLinden, M. O.; Klein, S. A.; Lemmon, E. W.; Peskin, A. P. REFPROP-Thermodynamic and Transport Properties of Refrigerant and Refrigerant Mixtures. *NIST, Standard Reference Database 23*, version 7; NIST: Gaithersburg, MD, 2002.
- (26) McLinden, M. O.; Lemmon, E. W.; Scott, J. NIST, private communication, 2001.
- (27) Ribeiro, A. P. C. Estrutura e Propriedades Dieléctricas de Refrigerantes Ambientalmente Aceitáveis. M.Sc. Thesis, Faculty of Sciences, University of Lisbon, 2007; pp 43–45.

Received for review June 15, 2007. Accepted July 20, 2007. This work was partially funded by the Pluriannual Funding to Centro de Ciências Moleculares e Materiais from Fundação para a Ciência e a Tecnologia, Portugal

JE700343T